New Approach to Total Dose Specification for Spacecraft Electronics

Michael Xapsos

***Abstract*—Variability of the space radiation environment is investigated with regard to total dose specification for spacecraft electronics. It is shown to have a significant impact. A new approach is developed for total dose requirements that replaces the radiation design margin concept with failure probability during a mission.**

I. Introduction

Hardness assurance (HA) methodology should ensure that electronic piece parts in a space system perform to design specifications after exposure to the space environment. Detailed descriptions of radiation HA methodology have been given in the 2002 and 2004 Nuclear and Space Radiation Effects Conference Short Courses [1], [2], and elsewhere [3]. Fig.1 shows an overview of the radiation HA process used at NASA Goddard Space Flight Center (GSFC), taken from reference 1. Starting from the mission requirements there are two branches of analysis that feed into parts categorization, describing their acceptability for flight. This is currently based on radiation design margin (*RDM*). The *RDM* is defined as the mean of the radiation failure level of the part, R_{mf}, divided by the radiation specification level derived from the environment, R_{spec}.

$$RDM = \frac{R_{mf}}{R_{spec}} \quad (1)$$

Determining the mean failure level of a part generally requires analysis of the lot or lots of devices to be flown along with system and circuit design to define a distribution of total dose failure levels. On the other hand, the radiation specification level, i.e., total dose level determined from the space environment, is taken as a fixed quantity even though the radiation environment is dynamic and must be predicted years in advance in order to incorporate requirements into the mission design. The reason behind this is largely historical. It results from the deterministic nature of the long-time standard Aerospace Proton Model-8/Aerospace Electron Model-8 (AP8/AE8) trapped particle models that are used to evaluate the total dose environment within the Earth's magnetosphere [4], [5]. In contrast, the new AP9/AE9 models are probabilistic in nature. They allow full Monte Carlo calculations for evaluating the dynamics of the trapped particle environment [6]. This is consistent with widely used solar proton models, which take the probabilistic approach [7]-[9]. Making use of probabilistic models for both trapped particles and solar protons allows the complete probability distribution of total dose values for any orbit to be evaluated for the first time. This provides additional useful information to designers because the environment variability is fully quantified. The new information can be inserted into the flow of the radiation HA process in the upper right box shown in Fig.1 to provide a more complete and consistent analysis for parts categorization. Parts categorization is central to radiation HA methodology because it determines part acceptability and whether or not lot acceptance testing should be performed.

Section II shows how the probability distribution for total dose failure of a lot(s) of devices is combined with the probability distribution of possible total dose values during a planned mission to obtain a predicted device failure probability during the mission. The end result is that use of this failure probability replaces the use of *RDM*. Examples for both total ionizing dose (TID) and displacement damage dose (DDD) are given. Section III discusses implications for radiation HA. Section IV presents conclusions.

II. Methods and Results

A. Derivation of Failure Probability during a Mission

Suppose one or more similar lots of devices is total dose tested in a laboratory. *G(x)* is the measured cumulative distribution function (CDF) and $g(x)$ is the corresponding probability density function (PDF) for failure doses of the devices. The probability of device failure for a dose that lies between *x* and *x* + *dx* is therefore $g(x)dx$, where the dose *x* is determined by experiment. The driving physical factors behind the space radiation environment are not entirely understood, making it challenging to predict ahead of time. Thus, when designing for a space mission it is useful to model this dynamic environment probabilistically. If the CDF for the space radiation dose is given by *H(x)* and the PDF is *h(x)*, then the probability a device is exposed to a dose that exceeds *x* during the mission is 1 – *H(x)*. A common assumption in the radiation effects community is that dose is a valid parameter for predicting device failure, i.e., a unit dose in the laboratory

Manuscript submitted May 19, 2017. This work is supported by the NASA Living With a Star Space Environment Testbed Program.

M.A. Xapsos is with NASA Goddard Space Flight Center, Greenbelt, MD, 20771 USA (Michael.A.Xapsos@nasa.gov; ph: (301)-286-2263; fax: (301)-286-4699).

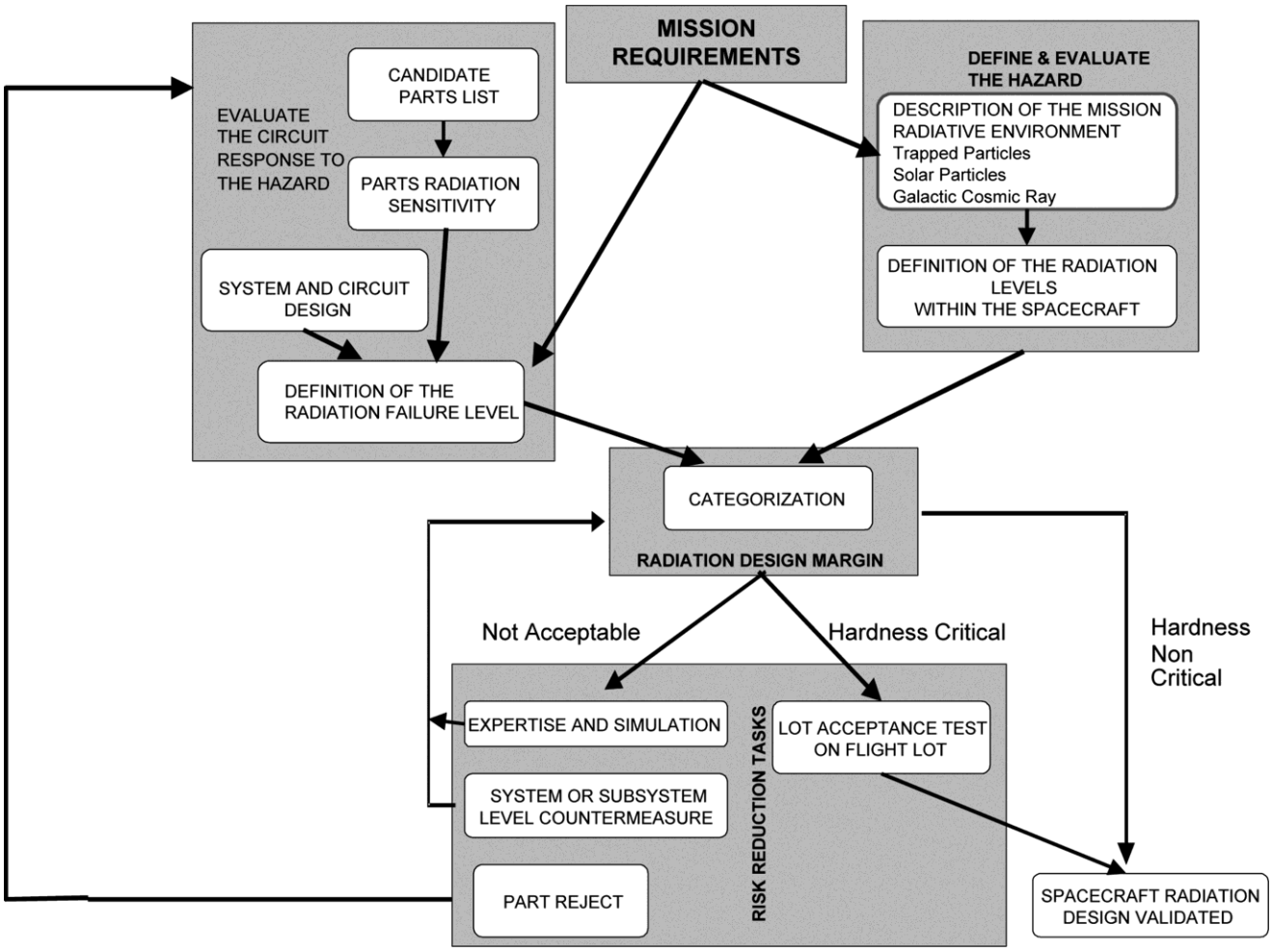

Fig. 1. Overview of the radiation hardness assurance process, taken from C. Poivey [1].

is equivalent to a unit dose in space. For situations where differences may occur such as devices subject to enhanced low dose rate sensitivity (ELDRS) or annealing, it is assumed the laboratory tests are done in a manner to accurately represent the failure distribution expected in the space radiation environment. This can often be accomplished by testing at an appropriately low dose rate but other approaches also exist that can potentially bound or approximate the low dose rate response [10], [11].

These two distributions can then be combined to obtain the probability for a total dose failure during the mission for dose interval *x* to *x* + *dx*. It is

$$[1 - H(x)] \cdot g(x)dx \tag{2}$$

Integrating over all possible dose values gives the total dose failure probability, P_{fail}, during the mission.

$$P_{fail} = \int [1 - H(x)] \cdot g(x)dx \tag{3}$$

To be clear, P_{fail} is the probability of a total dose failure for a device randomly selected from the lot(s) characterized by *G(x)* in the space environment characterized by *H(x)*. The failure can be either due to TID or DDD, depending on the device vulnerability.

B. Device Total Dose Failure Distribution, G(x)

Piece-part failure can be defined in terms of parametric or functional failure. In the examples considered here parametric failures are used. This generally requires circuit analysis to identify the most critical parameters for system operation. Standard methods for determining the dose failure distributions have been described in detail [1]-[3] as well as new methods that use Bayesian statistics [12] and techniques for building large data sets [13]. Adding to this particular literature is beyond the scope of this paper. The illustrative examples shown here were obtained by the standard method outlined by Pease for fitting a lognormal distribution to the failure levels of a lot(s) of devices [2].

Fig.2 shows degradation of DC current gain as a function of ionizing dose for Solid State Devices, Inc. SFT2907A bipolar transistors. These devices are used for high speed, low power applications and were tested for the Magnetospheric MultiScale (MMS) flight project. Ten devices from a single lot date code were irradiated using the gamma ray facility at NASA/GSFC to a total dose of 100 krad(Si), with an additional device used as a control. Results shown here for DC current gain are with a 10 V collector-emitter bias and 1 mA collector current.

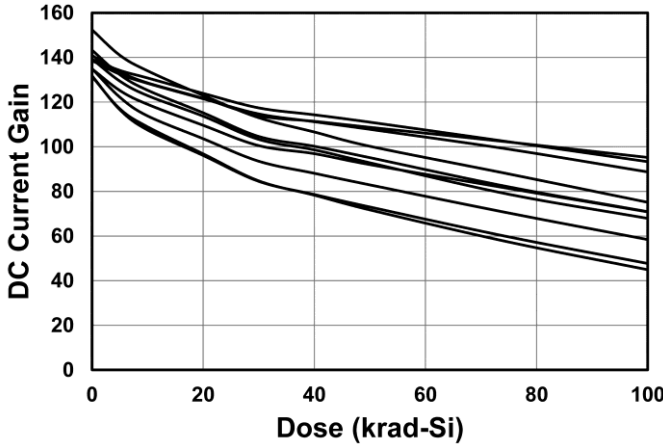

Fig. 2. DC current gain degradation as a function of Co-60 gamma ray dose for ten Solid State Devices, Inc. SFT2907A bipolar transistors.

Parametric failure occurs when the space system no longer operates properly because the transistor gain has degraded to a certain level. Under the test conditions described for Fig.2 it is assumed that parametric failure occurs at the dose where the gain falls below the manufacturer's minimum specification of 100. The failure distribution for the 10 devices was then put in the form of a cumulative probability by ranking the failure doses from 1 to 10 and dividing the rank, *m*, by *N + 1*, where *N* is the number of devices. The results are shown by the points in Fig.3. The points were then fit to a lognormal distribution shown by the line in the figure. This fit represents the CDF, *G(x)*, where *x* is TID. The correlation coefficient of the fit is 0.981. Since the lognormal parameters are now known they can be used to obtain the PDF, $g(x)$, used in equation 3.

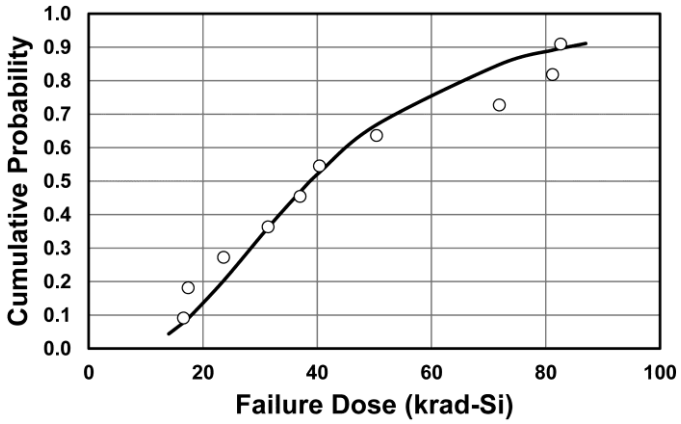

Fig. 3. TID failure distribution for the SFT2907A bipolar transistor. The line is a lognormal fit to the data.

For the situation where parts have a guaranteed hardness level it may not be necessary to test. In that case *G(x)* can be taken as a step function with the 0 to 1 probability transition at the guaranteed hardness level.

Next a DDD failure distribution for the Amptek, Inc. HV801 optocoupler is obtained. This is a high voltage commercial part rated for 8 kV operation of the detection photodiode. These are GaAlAs parts manufactured in a liquid phase epitaxially grown process. The data were taken by the Jet Propulsion Laboratory group for the JUpiter Near-polar Orbiter (Juno) flight project. Experiments using 50 MeV protons at the University of California, Davis Cyclotron Facility resulted in the degradation of current transfer ratio (CTR) shown in Fig.4. Experiments with Co-60 gamma rays showed no measureable effect on the optocouplers. It is therefore assumed that the CTR degradation is due to displacement damage in the Light Emitting Diode (LED) [14]. Parametric failure is taken as the point where the CTR degrades to 0.01.

The conversion of proton fluence to DDD is given by

$$DDD = C \cdot NIEL \cdot \phi \qquad (4)$$

where *NIEL* is the non-ionizing energy loss [15] for 50 MeV protons in GaAlAs, ϕ is the proton fluence and C is a unit conversion. The NIEL value used was 4.044 x 10^{-3} MeV-cm^2/g. For fluence expressed in units of cm^{-2} and C taken as unity, DDD is in units of MeV/g. In an analogous fashion to that shown in Fig.3 the DDD failure levels of the 6 parts can be ranked and plotted as a cumulative probability. This is shown by the points in Fig.5. A lognormal distribution was fit to these data and shown by the line in the figure. The correlation coefficient of the fit is 0.930. This is taken as the failure distribution, *G(x)*, where *x* is DDD.

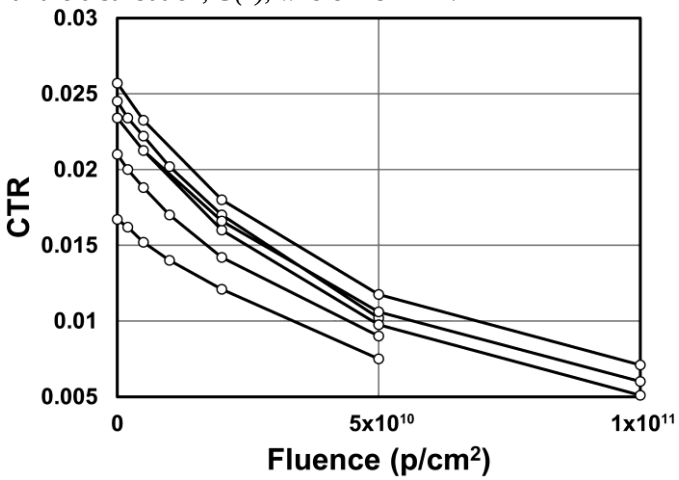

Fig. 4. CTR degradation for the HV801 optocoupler as a function of 50 MeV proton fluence. For clarity, the top curve has its CTR incremented by 0.002 at each data point.

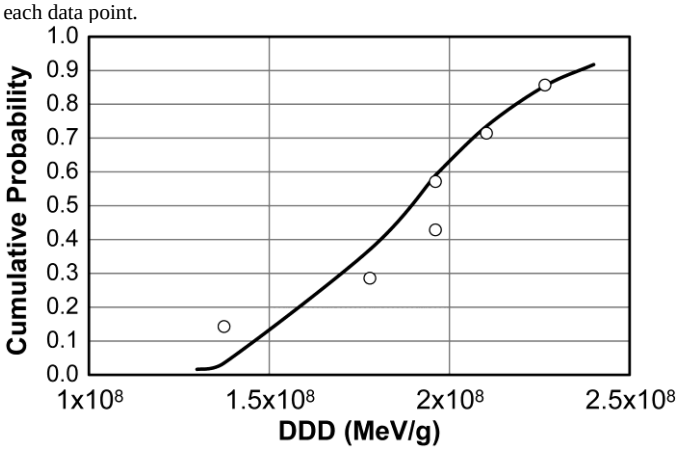

Fig. 5. DDD failure distribution for the HV801 optocoupler. The line is a lognormal fit to the data.

TABLE I
Orbits analyzed and corresponding radiation models used.

Orbit	Altitude (km)	Inclination	Duration	Comments	Models Used
Low Inclination LEO	569	28.5°	1 year	HST Orbit	AP9, AE9
Polar LEO	705	98.2°	1 year	Landsat-8 Orbit	AP9, AE9, ESP
GEO	35,786	0°	1 & 10 years	0° longitude	AP9, AE9, ESP

C. Space Radiation Environment Dose Distribution, H(x)

In order to evaluate the failure probability of a device during a mission as expressed by equation 3, the dose that the device will receive in space should be described probabilistically. There are many possibilities in terms of orbits and mission duration combinations. Three illustrative orbits in the near-Earth region are considered that have significantly different radiation environments. The first is a low-inclination, low Earth orbit (LEO). Here spacecraft are exposed to trapped protons in the South Atlantic Anomaly, and trapped electrons but are well-shielded from solar protons by the geomagnetic field. This is an orbit with moderate total dose exposure. The orbital altitude and inclination chosen were those of the Hubble Space Telescope (HST). Next a polar LEO or sun synchronous orbit is considered. Doses are somewhat more severe in this orbit because the trapped electron flux is greater and the spacecraft is only partially protected from solar protons. The altitude and inclination were chosen to match that of the Landsat-8 spacecraft. Thirdly, a geostationary Earth orbit (GEO) was chosen. This orbit is exposed to the intense outer electron belt and solar protons that are essentially unattenuated by the Earth's magnetic field. In GEO there are also trapped protons but they are stopped by very light shielding due to their low energy at this altitude.

All three orbits were examined for a 1-year mission duration for baseline comparisons. In addition the GEO was evaluated for a 10-year mission duration in order to assess the device failure probabilities for a longer period of time that is more appropriate for many GEO missions. The radiation models used were AP9/AE9 [6] and Emission of Solar Protons (ESP) [9]. For the case of the polar LEO solar proton attenuation was accounted for using the Magnetocosmics simulation as implemented in the Space Environment Information System (SPENVIS) [16]. A summary of the orbital information and radiation models used for each environment is given in Table I.

The AP9/AE9 Monte Carlo code, version 1.30, was used to simulate 99 histories for each orbit and mission duration combination. The orbit generator was run for the full mission length in all cases, either 1 or 10 years, to account for space weather variability built into the Monte Carlo version of the code. Time steps chosen were either 10 seconds for LEO or 1 hour for GEO. Resulting energy spectra for protons and electrons were transported through solid sphere aluminum shielding ranging from 10 to 1000 mils using the Numerical Optimizations, Visualizations, and Integrations on Computer Aided Design (CAD)/Constructive Solid Geometry (CSG) Edifices (NOVICE) radiation transport code [17]. Transported spectra were then converted to TID and DDD. The resulting doses for protons and electrons were then separately ranked by percentile according to $m/(N+1)$, where m is the ordered rank of the dose and N the number of histories. This allows both the trapped proton doses and trapped electron doses to be ordered from the 1 to 99 percentile or confidence level. Solar proton doses, both TID and DDD, were calculated with the ESP model and the NOVICE transport code for each integral percentile ranging from 1 to 99. The doses for trapped protons, trapped electrons and solar protons were then added for the same confidence level and shielding thickness.

Figs.6 and 7 show TID results for the 1-year low inclination LEO and 1-year GEO missions. Each curve represents the function $H(x)$ for a specified shielding level. Under lightly shielded conditions the doses expected for the GEO orbit are 2 to 3 orders of magnitude higher, depending on confidence level. However, the doses in this electron dominated orbit fall off quickly with increased shielding and become more comparable to the LEO under heavily shielded conditions. The width of the distributions shown represents the TID variability for all significant ionizing radiation in these orbits. It is noteworthy that the distribution width is comparable to the width of the failure distribution shown in Fig.3, showing the importance of environment variability for TID.

Figs.8 and 9 show DDD results for the same two orbits. These results are used in equation 3 for the function $H(x)$. Compared to the ionization case, the difference in DDD is much less for the two orbits under lightly shielded conditions. The main reason is that electrons, which dominate the GEO environment, are not efficient at producing displacements due to the large mismatch in mass with the GaAlAs target elements. DDD in GEO is more easily shielded against, as can be seen in Fig.9 by the translation of the curves leftward with increased shielding as compared to Fig.8. However, it is interesting to note the broad increase in the distribution width for GEO, particularly at high levels of shielding. There are at least two contributing factors that can be seen from equation 4. The first is that the electron fluence reaching a given shielding depth is highly statistical due to the large scattering angles electrons can be deflected at when interacting with a target atom. This can also be seen to a limited extent in Fig.7 for the case of ionization. The more significant reason is that the electron must have at least a few hundred keV of kinetic energy to displace an atom so electron NIEL consequently drops sharply for energies below about 1 MeV [15]. The resulting statistics of displacement damage energy loss in this energy region lead to a broad distribution for the high shielding levels considered. Figs. 8 and 9 show the DDD variability for all radiations that contribute significantly to displacement damage in these orbits. Note that depending on the level of shielding the width of the distribution can be much broader than the width of the failure distribution shown in

Fig.5, indicating the importance of environment variability for DDD.

The polar LEO results turned out to be intermediate to the other two orbits, as expected. This will be discussed in the following section along with results for the 10-year GEO.

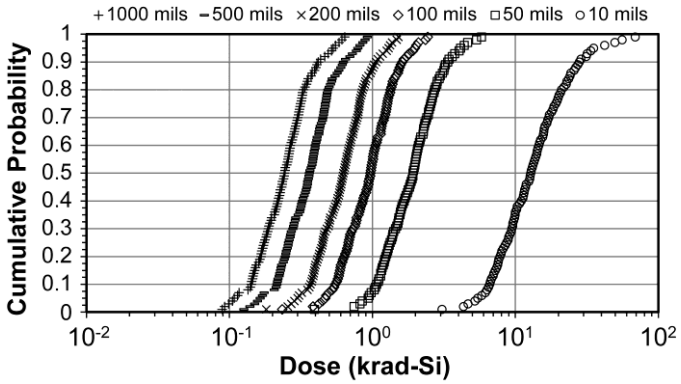

Fig. 6. TID probability distributions for a 1-year low inclination LEO mission. Each curve contains 99 points corresponding to confidence levels ranging from 1 to 99%. Shielding levels for the curves, from right to left, are 10, 50, 100, 200, 500 and 1000 mils Al. See Table I for orbital parameters.

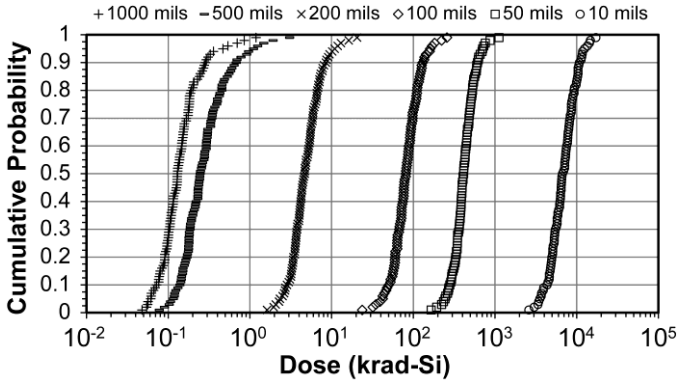

Fig.7. TID probability distributions for a 1-year GEO mission. Each curve contains 99 points corresponding to confidence levels ranging from 1 to 99%. Shielding levels for the curves, from right to left, are 10, 50, 100, 200, 500 and 1000 mils Al. See Table I for orbital parameters.

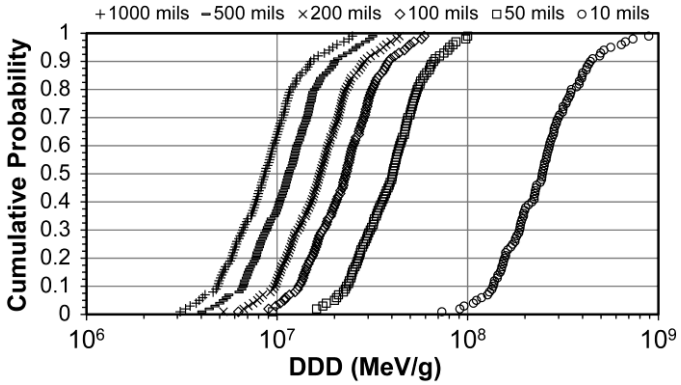

Fig. 8. DDD probability distributions for a 1-year low inclination LEO mission. Each curve contains 99 points corresponding to confidence levels ranging from 1 to 99%. Shielding levels for the curves, from right to left, are 10, 50, 100, 200, 500 and 1000 mils Al. See Table I for orbital parameters.

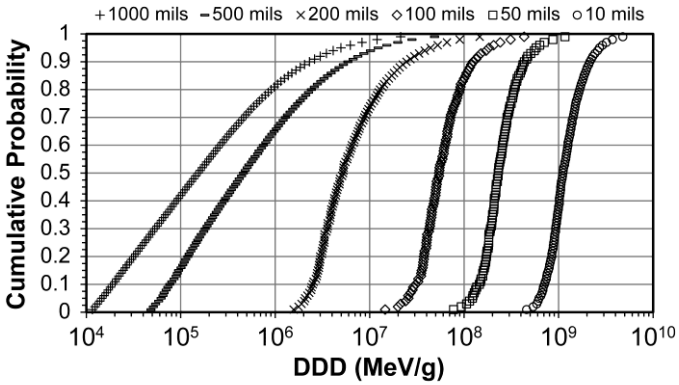

Fig.9. DDD probability distributions for a 1-year GEO mission. Each curve contains 99 points corresponding to confidence levels ranging from 1 to 99%. Shielding levels for the curves, from right to left, are 10, 50, 100, 200, 500 and 1000 mils Al. See Table I for orbital parameters.

D. Total Dose Failure Probability during a Mission

The failure probability for a device during a mission can now be calculated. For the bipolar devices this is done by combining the probability distribution for device failure shown in Fig.3 with a space radiation dose distribution for a given orbit and level of shielding such as those shown in Figs.6 and 7, using equation 3. The resulting failure probability, P_{fail}, depends on the proximity of the two distributions along the dose axis. If the device failure distribution is at much greater doses than the environment dose distribution the failure probability is 0. Conversely if the environment dose distribution is at much greater doses the failure probability is 1. When the two distributions overlap the failure probability is between 0 and 1.

Failure probabilities for the bipolar transistor are shown in Fig.10 as a function of shield thickness for all orbits and mission durations indicated in Table I. These were obtained by numerically integrating equation 3 using the appropriate probability distributions. It is seen that for 1-year missions the transistors should have at least 25, 50 and 200 mils of aluminum shield in low inclination LEO, polar LEO and GEO, respectively, to lower the failure probability to near zero. In order to extend the GEO mission from 1 to 10 years approximately 100 mils of additional shielding is required to maintain P_{fail} near 0.

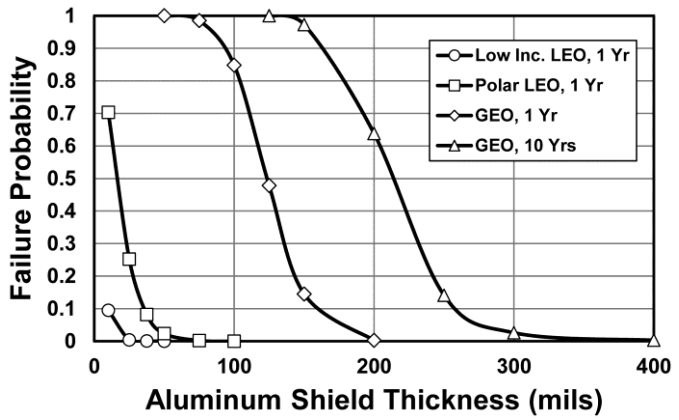

Fig. 10. Failure probabilities for the SFT2907A bipolar transistor as a function of shield thickness for different orbits and mission durations.

Fig.11 shows the failure probabilities for the HV801 optocoupler calculated in an analogous manner using DDD as the variable *x* in equation 3. The same general trends are seen for the different orbits considered. It is interesting to note that the resulting curves from the last two figures provide a ranking of the severity of threats for different devices, regardless of whether it is due to TID or DDD.

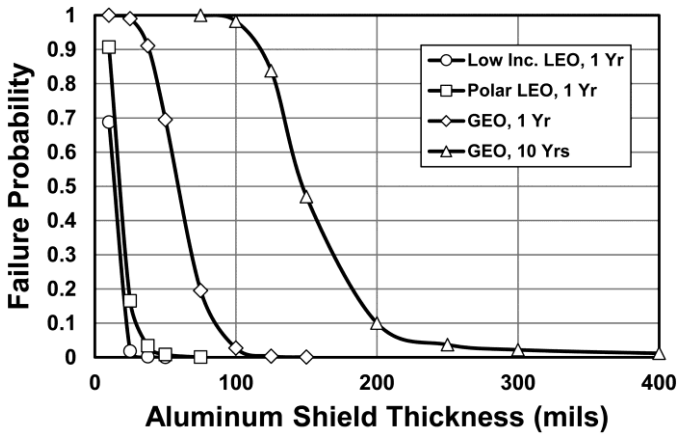

Fig. 11. Failure probabilities for the HV801 optocoupler as a function of shield thickness for different orbits and mission durations.

III. Discussion – Radiation Hardness Assurance

The two generally accepted radiation analyses that lead to part categorization shown in Fig.1 have been discussed. First the distribution of part failures due to total dose is accounted for. Second the total dose space environment is analyzed. Until recently the available space radiation environment tools did not have the capability to allow this to be done on a consistent basis. The environment has typically been evaluated by combining results from deterministic trapped particle models and probabilistic solar proton models. This leads to a total dose value for a specified shielding and assignment of an arbitrary *RDM* to account for its uncertainty. However, the dynamic nature of the environment and the need to forecast it years in advance suggests a probabilistic approach is preferable. The availability of the AP9/AE9 Monte Carlo code, when combined with a probabilistic solar proton model, now allows a more consistent approach to be taken. As shown in section II, this results in modifying parts categorization by replacing *RDM* with failure probability, P_{fail}. P_{fail} represents the probability of a total dose failure during a mission for a device randomly selected from the lot(s) to be flown, accounting for the distribution of possible total dose environments. It is free of the arbitrariness of choosing an *RDM*.

The *RDM* has a long history of use in the radiation effects community. It is therefore worthwhile to compare *RDM* with confidence level for a given environment. This can be done using figures such as 6 – 9 if the assumption is made that the 50% confidence level is equivalent to an *RDM* of 1. Values of *RDM* greater than 1 are then obtained by taking the ratio of the dose at the confidence level of interest to the dose at the 50% confidence level. This applies to both TID and DDD. Comparisons are shown in Fig.12 for the 10-year GEO, which is the most challenging orbit for total dose requirements considered in this paper. Results are for a shielding level of 200 mils of aluminum, a reasonable starting point for a large spacecraft intended for a 10-year mission in GEO. A commonly applied *RDM* is a factor of 2, although this varies across organizations and even for particular applications. The figure shows that for the case of ionization this corresponds to a high confidence level, approximately 96%. This is expected, as part selection for total dose effects is generally quite conservative. For the case of DDD an *RDM* of times 2 corresponds to a confidence level of about 79%. This is less than the ionization case because of the broadness of the DDD distributions in GEO, as shown in Fig.9. This reflects the inconsistency and the "catch-all" nature of *RDM*, which is used to cover uncertainties in both the environment and the device failure distribution for various applications. Difficulties can arise because environment uncertainties are dependent on the particular orbit, mission duration and environment dynamics. In addition the piece part failure distribution can vary significantly from a mean failure level and is not accounted for by equation 1 [18].

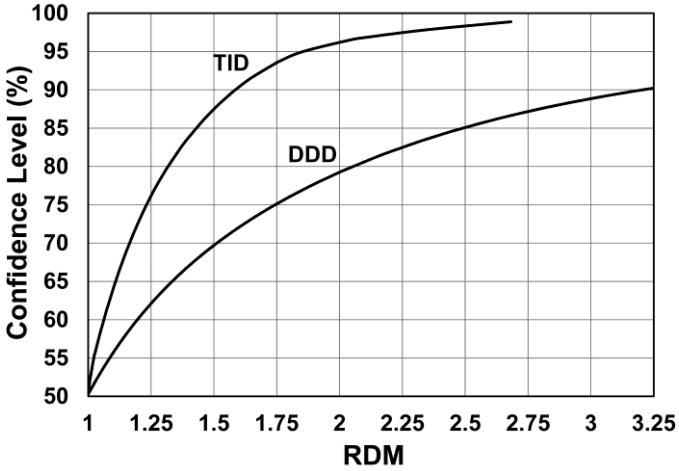

Fig. 12. Comparison of confidence level using the current methodology to *RDM* for a 10-year mission in GEO and 200 mils of Al shielding. Results are shown for both TID and DDD.

Changing over from an *RDM*- to a P_{fail}-based approach has favorable implications at the system and spacecraft level because the failure probability is more directly related to the reliable operation of a circuit than design margin. This would allow total dose failures to be included in spacecraft level reliability analyses as part of an overall probabilistic model, a procedure not currently being implemented at NASA.

The exact level of acceptable failure probability will be related to the risk the flight project is willing to take. This in turn is related to many factors such as whether the mission is manned or robotic, mission goals and cost.

IV. Conclusions

An approach was presented that accounts for the variability of the space radiation environment in total dose hardness assurance methodology. Two example applications were demonstrated using bipolar transistor and

optocoupler data. Although other devices need to be considered on a case-by-case basis, the results obtained showed that variability in the total dose space environment was at least as significant as the variability of the device failure distributions obtained from laboratory tests, suggesting this approach provides a more complete and thorough radiation HA analysis. The main improvements in this approach are two-fold. First, the full probabilistic nature of each space radiation model is used, leading to a more consistent assessment of the radiation environment in terms of confidence levels across all radiations. Second, parts categorization is accomplished by evaluating failure probability, P_{fail}, instead of *RDM*. The advantages of using failure probability are that it is an objectively determined parameter that better characterizes device radiation performance. It allows direct comparison of the total dose threats for different devices, regardless of whether it is TID or DDD. Finally, it is more amenable to circuit, system and spacecraft reliability analyses.

REFERENCES

[1] C. Poivey, "Radiation Hardness Assurance for Space Systems," in 2002 IEEE NSREC Short Course Notebook: *Radiation Effects – From Particles to Payloads*, IEEE Publishing Services, Piscataway, NJ, pp. V1-V57.

[2] R. Pease, "Microelectronic Piece Part Radiation Hardness Assurance for Space Systems," in 2004 IEEE NSREC Short Course Notebook: *Hardness Assurance and Photonic Challenges for Space Systems*, IEEE Publishing Services, Piscataway, NJ, pp. II1-II56.

[3] R. Pease and D. Alexander, "Hardness Assurance for Space System Microelectronics," *Radiat. Phys. Chem*., vol. 43, no. 1-2, pp. 191-204, 1994.

[4] D.M. Sawyer and J.I. Vette, "AP-8 Trapped Proton Environment for Solar Maximum and Solar Minimum," NASA/GSFC, Greenbelt, MD, USA, NSSDC/WDC-A-R&S, 76-06, 1976.J.I. Vette, "The AE-8 Trapped Electron Model Environment," NASA/GSFC, Greenbelt, MD, USA, NSSDC/WDC-A-R&S, 91-24, 1991.

[5] G. Ginet et al., "The AE9, AP9 and SPM: New Models for Specifying the Trapped Energetic Particle and Space Plasma Environment," *Space Sci. Rev*., vol. 179, issue 1-4, pp. 579-615, Nov. 2013.

[6] J.H. King, "Solar Proton Fluences for 1977-1983 Space Missions," *J. Spacecraft*, vol. 11, pp. 401-408, 1974.

[7] J. Feynman, G. Spitale, J. Wang and S. Gabriel, "Interplanetary Fluence Model: JPL 1991," *J. Geophys. Res*., vol. 98, pp. 13281-13294, 1993.

[8] M.A. Xapsos, G.P. Summers, J.L. Barth, E.G. Stassinopoulos and E.A. Burke, "Probability Model for Cumulative Solar Proton Event Fluences," *IEEE Trans. Nucl. Sci.*, vol. 47, no. 3, pp. 486-490, June 2000.

[9] D.M. Fleetwood and H.A. Eisen, "Total-Dose Radiation Hardness Assurance," *IEEE Trans. Nucl. Sci.*, vol. 50, no. 3, pp. 552-564, June 2003.

[10] R.L. Pease, R.D. Schrimpf, and D.M. Fleetwood, "ELDRS in Bipolar Linear Circuits: A Review," *IEEE Trans. Nucl. Sci.*, vol. 56, no. 4, pp. 1894-1908, Aug. 2009.

[11] R. Ladbury and B. Triggs, "A Bayesian Approach for Total Ionizing Dose Hardness Assurance," *IEEE Trans. Nucl. Sci*., vol. 58, no. 6, pp. 3004-3010, Dec. 2011.

[12] R. Ladbury and M.J. Campola, "Statistical Modeling for Radiation Hardness Assurance: Toward Bigger Data," *IEEE Trans. Nucl. Sci*., vol. 62, no. 5, pp. 2141-2154, Oct. 2015.

[13] K.A. LaBel et al., "A Compendium of Recent Optocoupler Radiation Test Data," in *2000 IEEE Rad. Eff. Data Workshop Record*, pp. 123-146.

[14] G.P. Summers, E.A. Burke, P. Shapiro, S.R. Messenger and R.J. Walters, "Damage Correlations in Semiconductors Exposed to Gamma, Electron and Proton Radiations," *IEEE Trans. Nucl. Sci*., vol. 40, no. 6, pp. 1372-1379, Dec. 1993.

[15] SPENVIS. Available: https://www.spenvis.oma.be/intro.php

[16] T.M. Jordan, "An Adjoint Charged Particle Transport Method," *IEEE Trans. Nucl. Sci*., *v*ol. 23, no. 6, pp. 1857-1861, Dec. 1976.

[17] R. Ladbury, J.L. Gorelick and S.S. McClure, "Statistical Model Selection for TID Hardness Assurance," *IEEE Trans. Nucl. Sci*., vol. 56, no. 6, pp. 3354-3360, Dec. 2009.